International Journal of General Medicine

Dovepress
Taylor & Francis Group

Open Access Full Text Article

ORIGINAL RESEARCH

# The Improved-EFI Score: A Multi-Omics-Based Novel Efficacy Predictive Tool for Predicting the Natural Fertility of Endometriosis Patients

Qiumin He[1,*], Chongyuan Zhang[2,*], Yao Hu[1], Jinfang Deng[1], Shuirong Zhang[1]

[1]Department of Gynaecology,Jingzhou Central Hospital, Jingzhou Hospital Affiliated to Yangtze University, Jingzhou, Hubei, 434020, People's Republic of China; [2]Department of Gynaecology,Jingzhou Maternal and Child Health Hospital, Jingzhou, Hubei, 434000, People's Republic of China

*These authors contributed equally to this work

Correspondence: Shuirong Zhang, Email zhangshuirong1024@163.com

**Objective:** Infertility caused by endometriosis (EM) directly affects the possibility of pregnancy in women of gestational age. This study aims to establish a prediction model to accurately predict the natural pregnancy outcome of patients with EM, providing valuable information for clinical decision-making.

**Methods:** We retrospectively selected a total of 496 patients who underwent their first laparoscopic surgery for infertility at the Obstetrics and Gynecology Department of Jingzhou Central Hospital from January 2016 to June 2023. An improved endometriosis fertility index (EFI) predictive model was created based on ultrasound radiomics and urinary proteomics gathered during the patient's initial admission, using two machine learning algorithms. The predictive model was evaluated for C-index, calibration, and clinical applicability through receiver working characteristic curve, decision curve analysis.

**Results:** The improved EFI prediction model nomogram, based on five ultrasound radiomics parameters and three urine proteomics, had AUC values of 0.921 (95% CI: 0.864–0.978) and 0.909 (95% CI: 0.852–0.966) in the training and validation sets, respectively, while the traditional EFI prediction model had AUC values of 0.889 (95% CI: 0.832–0.946) and 0.873 (95% CI: 0.816–0.930) in the training and validation sets, respectively. Additionally, the nomogram exhibited better discrimination ability and achieved an overall better benefit against threshold probability than the EFI model and decision tree in the decision curve analysis (DCA).

**Conclusion:** The combined ultrasound radiomics–urine proteomics model was better able to predict natural pregnancy-associated patients with EM compared to the classical EFI score. This can help clinicians better predict an individual patient's risk of natural pregnancy following a first-ever laparoscopic surgery and facilitate earlier diagnosis and treatment.

**Keywords:** endometriosis, infertility, Endometriosis Fertility Index, radiomics, uromics, prediction

## Introduction

Endometriosis (EM), as a benign gynecological disease in which endometrial glands and stroma appear outside the uterus, is most commonly found in the ovaries and uterosacral ligaments in clinical practice.[1–3] From the etiology of infertility, about one-third of infertile women are caused by EM.[4,5] Therefore, it is particularly important to eliminate the hidden dangers of infertility caused by EM and help achieve the expectation of natural conception during pregnancy. Up to now, the tools for clinical assessment of EM-related infertility risk still rely on the clinical staging of EM proposed by the American Society for Reproductive Medicine (ASRM) in 1979.[6,7] Although the ASRM staging was revised twice during the period, there was no significant correlation between the revised ASRM staging (rASRM) and the postoperative natural pregnancy rate.[8]

In 2010, Adamson et al proposed the Endometriosis Fertility Index (EFI) to predict the natural fertility rate of EM patients after surgery.[9,10] Indubitably, the EFI is a scoring system based on laparoscopic surgery, which poses risks of surgery related and postoperative ovarian reserve dysfunction. In clinical practice, for patients with r-ASRM assessed as

Received: 24 December 2024
Accepted: 12 February 2025
Published: 19 February 2025

stage III–IV, it is usually recommended that they actively undergo assisted reproductive technology.[11] Therefore, if EFI can be predicted before laparoscopic surgery, doctors can provide more objective consultation on fertility issues in patients diagnosed with EM. Fortunately, Tomasetti et al have proposed a preoperative EFI scoring system through prospective research, which can accurately estimate EFI based solely on clinical and imaging examination (ultrasound) data.[12] As a creatively constructed EFI evaluation system, it still needs to optimize and improve its predictive performance, especially in the exploration of improved EFI, in order to achieve unparalleled predictive ability, especially in the preoperative evaluation stage.

In recent years, ultrasound radiomics has shown significant application value in the field of gynecology, especially in the diagnosis and treatment of gynecological malignant tumors.[13] For example, ultrasound radiomics can provide detailed information about tumor heterogeneity and biological behavior by analyzing the imaging features of tumors, such as shape, texture, intensity, etc.[14,15] This is particularly important for preoperative evaluation of malignant tumors, as it can help doctors more accurately determine the invasiveness of the tumor and predict high-risk factors such as lymph node metastasis and parametrial invasion.[16] In fact, ultrasound radiomics has shown great potential in the diagnosis and treatment of EM, especially in extracting a large amount of image information from ultrasound images and combining it with artificial intelligence and other methods to provide additional information beyond what conventional ultrasound can explore, thereby improving the accuracy of ultrasound diagnosis. So far, although existing studies have not directly mentioned the application of ultrasound radiomics in the treatment of EM, the progress of radiomics in tumor treatment suggests that radiology may predict treatment outcomes by analyzing the ultrasound image features of tumors, thereby guiding treatment strategies. In addition, the application of urinary proteomics in EMs is mainly reflected in the analysis of differential proteins in urine through proteomics techniques to identify potential diagnostic markers and therapeutic targets.[17] Recent study has shown that histone 4 (H4) levels are elevated in the urine of patients with ovarian endometriosis, providing a new biomarker for early diagnosis of endometriosis.[18] However, it is still unknown whether urine proteomics has the potential to enhance natural pregnancy outcome prediction in patients with EM.

At present, there is not yet abundant studies on the combined application of ultrasound radiomics and urine proteomics for EM. But theoretically, the combination of these two methods may provide more comprehensive and accurate information for the diagnosis and treatment of EM. In this study, we will combine these two methods to help doctors potentially improve EFI prediction performance earlier and more accurately, and develop more personalized treatment plans.

# Materials and Methods

## Study Population

We retrospectively selected a total of 496 patients who underwent their first laparoscopic surgery for infertility at the Obstetrics and Gynecology Department of Jingzhou Central Hospital from January 2016 to June 2023. The selection criteria are as follows: (1) Patients who have had normal sexual activity for more than 1 year, have not used contraception, are not pregnant, and have been diagnosed with EM; (2) Admitted for gynecological three-dimensional ultrasound imaging examination, and the imaging data are complete; (3) Patients who retain qualified urine samples upon admission; (4) The patient is at least 20 years old and has signed a research informed consent form. Exclusion criteria: (1) Patients with postoperative pathological diagnosis of non EM, combined with adenomyosis and male factor infertility; (2) Other lesions that may lead to infertility, such as salpingitis secondary to pelvic infection or submucosal fibroids; (3) Patients with organic lesions such as liver and kidney dysfunction; (4) Patients who have undergone pelvic surgery before surgery or have been confirmed to have pelvic benign or malignant tumors; (5) Patients with incomplete or missing inpatient case information; (6) Patients who refuse to undergo three-dimensional ultrasound examination of the uterus or adnexa, or have incomplete or substandard ultrasound imaging data. This study has been approved and agreed to be conducted by the Medical Ethics Committee of Jingzhou Central Hospital. All patients included in this study are aware of and have signed informed consent forms, and strictly comply with the Helsinki Declaration. The patient inclusion and prediction model construction are shown in Figure 1.

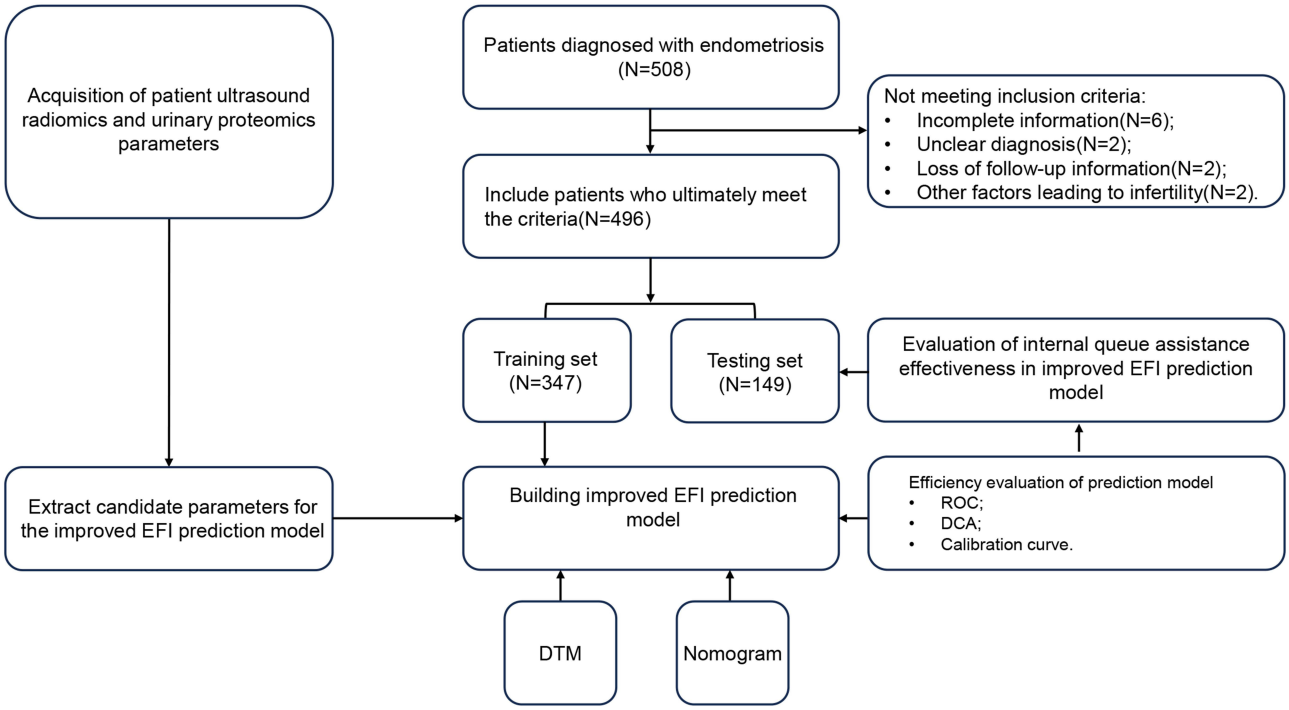


**Figure 1** Flowchart for screening and constructing prediction models for the included population.

## Definition of Postoperative Natural Conception

The patients included in this study are all women of childbearing age, ranging from 20 to 45 years old. All patients underwent laparoscopic minimally invasive surgery and attempted natural preconception. Usually, ultrasound examination can show clear gestational sacs and fetal buds in the uterus, and pregnancy can be confirmed through human chorionic gonadotropin (HCG) testing in blood. If HCG levels are elevated and there are gestational sacs and fetal heartbeats visible in the uterine cavity through ultrasound, it is usually considered a successful clinical pregnancy.

## Texture Capture and Parameter Extraction in Radiomics

We use the S2000 ultrasound diagnostic instrument from Siemens in Germany, with the probe detection frequency set to 4–9 MHz. All patients underwent routine ultrasound examination of the uterine adnexa within 1 week before surgery. They were placed in a supine position and multiple sections of ovarian chocolate cysts were scanned to observe the nodules. On the basis of good-quality two-dimensional ultrasound images of the nodules, the largest section of the nodules was stored, and the images were stored in DICOM format on the hard drive. Two physicians with over 5 years of experience in gynecological ultrasound diagnosis applied the ITK-SNAP 3.8 software to manually delineate the region of interest (ROI) along the approximate contour of the ovarian cyst on ultrasound image, under the premise of unknown pathological examination results. Then, the texture capture area was automatically expanded outward by 2 mm based on the boundary delineated by the intra tumor ROI. Pyradiomics software is applied to extract radiomics features from the delineated ROI region, which mainly includes four types of features: morphological features, first-order histogram features, texture features, and wavelet features. The texture features mainly include gray level run length matrix (GLRLM), gray level co-occurrence matrix (GLCM), gray level dependence matrix (GLDM), gray level size zone matrix (GLSZM), and neighborhood gray tone difference matrix (NGTDM).

The Z-score method was used to normalize the extracted ultrasound imaging omics features, followed by *t*-test, Pearson correlation analysis, and least absolute shrinkage and selection operator (LASSO) feature selection. The ultrasound imaging omics features with non-zero coefficients were selected using 10-fold cross-validation hyperparameters. After selecting the optimal features, an imaging omics support vector machine (SVM) model was constructed.


https://doi.org/10.2147/IJGM.S512359

According to the imaging omics score calculation formula Rad Score=X0+X1Y1+X2Y2+X3Y3+.+XnYn, the Rad Score score for each endometriotic cyst was calculated, where Yn represents the selected feature. The radiomics features of the ultrasound images are as follows: X0 is the constant of Rad Score, and Xn is the regression coefficient of the corresponding feature in the regression model.

## Urinary Proteomic Analysis and Biomarker Screening

The clinical samples were obtained after clinical urine routine testing, and the urine routine results were normal. The urine protein dry chemistry test was negative. After centrifugation at 3000 × g for 15 minutes, the supernatant was collected and frozen at −80 °C. We used an Orbitrap Exploris 480 mass spectrometer (Thermo Scientific, USA) coupled with an EASY nLC 1000 (Thermo Scientific, USA) chromatograph for data analysis in a dependent acquisition mass spectrometry mode. The digested peptides were separated on a RP C18 self filled capillary LC column (75 μm × 100 mm, particle size 3 μm), and the protein peptide segments were loaded in equal amounts. The elution gradient is 5%–30% buffer B2 (0.1% formic acid, 99.9% acetonitrile; flow rate, 0.3 μl/min), and the peptide was eluted for 25 minutes.

The raw data were collected independently and analyzed using default settings by Spectronaut Pulsar 17.1 (Biognosys, Switzerland). Set the retention time prediction type to dynamic index retention time. MS2 level interference correction has been enabled. The peptide intensity was calculated by summing the peak areas of the respective fragment ions of MS2, and the protein peak intensity was calculated by summing the intensities of the respective peptides. Enable cross-run normalization to correct system differences in liquid chromatography-mass spectrometry performance and use local normalization strategy. Protein inference was performed using the ID selector algorithm in Spectronaut. Filter all results using a Q cut-off value of 0.01 (corresponding to a false-positive detection rate of 1%). In this study, the HE4 (item number: SC-27570), ARF3 (item number: The antibodies sc-53167 and MYH10 (item number: sc-376942) were purchased from Sanying Co., Ltd.

## Development and Validation of Improved EFI Prediction Model

In order to reduce the bias caused by missing data, factors with missing values exceeding 20% were excluded during the data collection stage. Implement multiple imputation (MI) techniques to address missing values in residual variables for analysis. The MI method includes comprehensively considering the relationships between variables, assigning multiple reasonable values to missing entries, and generating multiple interchangeable datasets. Tenfold cross-validation was conducted to reduce overfitting and improve model stability. In the training set of patients, univariate logistic regression was used to determine variables that were independently correlated with the results. We then select a P-value cutoff value of 0.1 for feature selection.

We constructed preoperative EFI prediction models using two machine learning algorithms, namely generalized linear regression (GLRM) and decision tree (DT). Among them, the candidate variables selected by the generalized linear regression were analyzed through single factor and multiple factor regression, and the variables with a P-value less than 0.05 were finally included in the generalized linear regression model and presented as a nomogram visualization prediction model. The decision tree was pruned using the random forest iterative algorithm, which involved screening candidate variables at each branch node of the decision tree to be included in the final prediction model. Before constructing the machine learning EFI prediction model, a preliminary screening of ultrasound radiomics variables was conducted based on LASSO regression and Pearson correlation coefficient analysis, and the optimal combination of candidate variables was included in the final prediction model construction.

## Evaluation of the Efficiency of the Improved EFI Prediction Model

All patients underwent a modified EFI score before surgery and obtained a total score. Consistency prediction was made based on the preoperative modified EFI score and postoperative natural pregnancy outcomes. We used receiver operating characteristic (ROC) curves to evaluate the predictive ability of the model, calibration curves to evaluate the consistency between model prediction probability and sample probability, and decision curve analysis (DCA) to evaluate the clinical practicality of the model.

## Statistical Analysis

The data were analyzed and visualized using R software (version 4.2.2) and SPSS 26.0. Normal distribution and homogeneity of variance tests were performed on the quantitative data. Two-sample independent *t*-tests were conducted for those that followed a normal distribution. Mann–Whitney *U*-test was used to compare non-normal distribution continuous variables, and chi-square test was used to compare categorical variables. Logistic regression and decision tree are used to construct predictive models and plot ROC curves to obtain the accuracy, sensitivity, specificity, and area under curve (AUC) of the model. $P < 0.05$ indicates a statistically significant difference.

# Results

## Clinical Characteristics and Postoperative Natural Pregnancy Outcomes

As shown in Table 1, we analyzed the medical history information, clinical symptoms, physical examination, ultrasound results, and other aspects of all included patients and patients diagnosed with pathological results after surgery. A total of 496 EM patients were included in the final study. Among them, 179 EM patients failed to attempt natural conception after surgery (89 patients chose assisted reproductive technology for pregnancy), while another 317 EM patients successfully achieved natural conception within 1 year after undergoing laparoscopic surgery, including 11 (3.5%) chemical pregnancies and 8 (2.5%) ectopic pregnancies. In addition, based on the distribution of postoperative EFI scores, we found that 80.2% of the patients predicted EFI scores of 7–10 before surgery and 71.4% after surgery; The lowest proportion is in the low score range (0–4 points), accounting for 3.6% and 5.9% before and after surgery, respectively. Given this, we speculate that the higher EFI score may be related to the younger age and shorter duration of infertility in the included population.

## Screening of Additional EFI Score Candidate Feature

A total of 37 ultrasound-related omics features were obtained using PyRadiomics software, including 4 shape features, 8 first-order features, 4 gray level co-occurrence matrix features, 6 gray level region size matrix features, 6 gray level stroke matrix features, 5 neighborhood gray level difference matrix features, and 4 gray level correlation matrices. As shown in Figure 2A, five non-zero coefficient features were obtained through Spearman correlation, LASSO regression analysis for dimensionality reduction, and screening. Among them, two shape features reflect the spherical characteristics and surface area of the cyst; Two grayscale stroke matrix features and one grayscale region size matrix feature reflect the length non-uniformity, grayscale variance, and region entropy of the grayscale region size matrix of the cyst; The feature of a neighborhood grayscale difference matrix reflects the roughness of adjacent grayscale difference matrices in an image.

Next, we included variables with statistical differences between the natural pregnancy group and the non-natural pregnancy group in the training set into Lasso regression analysis. As the regularization parameter λ increased, the regression coefficients of each variable tended to zero, and the number of non-zero coefficient variables also decreased (Figure 2B). We drew vertical lines at the minimum value of λ (λ=0.014, Log λ=−3.619) and select one standard error of the minimum value of λ as the optimal value (Figure 2C), and screen out 10 non-zero coefficient predictive variables, including feature2, feature5, feature8, feature9, feature10, HE4, ARF3, and MYH10. Finally, SHAP analysis was conducted on the weight distribution of candidate variables in the generalized linear regression model and decision tree (Figure 2D and Supplementary Table 1).

## Construction of an Improved EFI Prediction Model Based on Nomogram

As shown in Table 2, among the four candidate features included, both univariate and multivariate logistic regression analyses showed significant statistical differences ($P<0.05$). So, we constructed a visual nomogram based on five candidate parameters (Figure 3A). Compared to traditional EFI scoring, the improved version of EFI scoring has been assigned new scores and weights, as well as additional ultrasound radiological parameters and urine proteomics. The total score was obtained based on the weight scores of each parameter in the nomogram, which was the improved EFI scoring. Furthermore, in order to evaluate the robustness of the improved EFI prediction model, we conducted 1000 resampling

https://doi.org/10.2147/IJGM.S512359



**Table 1** Clinical Characteristics and Omics Parameters of Patients With Endometriosis

| Variables | Training cohort | | | P-value | Testing cohort | | | P-value |
|---|---|---|---|---|---|---|---|---|
| | Overall (N=C) | Pregnancy (N=219) | Non-Pregnancy (N=128) | | Overall (N=149) | Pregnancy (N=98) | Non-Pregnancy (N=51) | |
| Age (median [IQR]),year | 32.00 [26.00, 39.00] | 32.00 [26.00, 39.00] | 32.00 [26.00, 40.00] | 0.932 | 32.00 [26.00, 40.00] | 32.00 [26.25, 40.00] | 31.00 [24.50, 38.00] | 0.23 |
| BMI (median [IQR]),kg/m2 | 22.70 [20.95, 25.40] | 22.70 [20.90, 25.30] | 22.75 [21.08, 25.42] | 0.761 | 22.80 [20.90, 25.10] | 22.65 [20.80, 25.20] | 23.20 [21.05, 25.05] | 0.845 |
| Sex (median [IQR]) | 11.00 [6.00, 15.00] | 11.00 [6.00, 15.00] | 10.50 [7.00, 15.00] | 0.886 | 11.00 [7.00, 15.00] | 12.00 [7.00, 14.75] | 11.00 [7.00, 17.00] | 0.646 |
| MP (median [IQR]),days | 7.00 [5.00, 10.00] | 7.00 [5.00, 9.00] | 7.00 [4.75, 10.00] | 0.766 | 7.00 [5.00, 9.00] | 7.00 [5.00, 9.00] | 7.00 [5.00, 10.00] | 0.315 |
| COD (median [IQR]),year | 4.00 [3.00, 6.00] | 4.00 [3.00, 6.00] | 4.50 [3.00, 6.00] | 0.959 | 4.00 [3.00, 6.00] | 4.00 [3.00, 6.00] | 5.00 [3.00, 7.00] | 0.094 |
| Dysmenorrhea (%) | | | | | | | | |
| Yes | 170 (49.0) | 104 (47.5) | 66 (51.6) | 0.534 | 71 (47.7) | 45 (45.9) | 26 (51.0) | 0.679 |
| No | 177 (51.0) | 115 (52.5) | 62 (48.4) | | 78 (52.3) | 53 (54.1) | 25 (49.0) | |
| LOL (%) | | | | | | | | |
| Unilateral | 176 (50.7) | 113 (51.6) | 63 (49.2) | 0.752 | 82 (55.0) | 55 (56.1) | 27 (52.9) | 0.844 |
| Bilateral | 171 (49.3) | 106 (48.4) | 65 (50.8) | | 67 (45.0) | 43 (43.9) | 24 (47.1) | |
| GI (%) | | | | | | | | |
| Yes | 176 (50.7) | 103 (47.0) | 73 (57.0) | 0.092 | 69 (46.3) | 45 (45.9) | 24 (47.1) | 1 |
| No | 171 (49.3) | 116 (53.0) | 55 (43.0) | | 80 (53.7) | 53 (54.1) | 27 (52.9) | |
| CS (%) | | | | | | | | |
| Yes | 171 (49.3) | 108 (49.3) | 63 (49.2) | 1 | 79 (53.0) | 48 (49.0) | 31 (60.8) | 0.231 |
| No | 176 (50.7) | 111 (50.7) | 65 (50.8) | | 70 (47.0) | 50 (51.0) | 20 (39.2) | |
| EFI (median [IQR]) | 7.00 [6.00, 9.00] | 9.00 [7.50, 9.00] | 5.00 [3.00, 6.00] | <0.001 | 7.00 [5.00, 9.00] | 8.00 [7.00, 9.00] | 4.00 [3.00, 5.00] | <0.001 |
| AMH (%),μg/L | | | | | | | | |
| <1 | 156 (45.0) | 80 (36.5) | 76 (59.4) | <0.001 | 64 (43.0) | 34 (34.7) | 30 (58.8) | 0.008 |
| ≥1 | 191 (55.0) | 139 (63.5) | 52 (40.6) | | 85 (57.0) | 64 (65.3) | 21 (41.2) | |
| Infertility (%) | | | | | | | | |
| Primary | 181 (52.2) | 111 (50.7) | 70 (54.7) | 0.543 | 78 (52.3) | 49 (50.0) | 29 (56.9) | 0.533 |
| Secondary | 166 (47.8) | 108 (49.3) | 58 (45.3) | | 71 (47.7) | 49 (50.0) | 22 (43.1) | |
| CA125 (median [IQR]), U/mL | 71.00 [49.00, 96.00] | 76.00 [48.00, 99.50] | 68.00 [49.75, 91.25] | 0.147 | 70.00 [48.00, 92.00] | 73.00 [49.25, 91.00] | 64.00 [45.00, 92.50] | 0.41 |
| Feature1 (median [IQR]) | 62.00 [37.00, 87.00] | 61.00 [36.50, 87.00] | 63.50 [37.00, 85.00] | 0.702 | 58.00 [34.00, 87.00] | 58.00 [31.25, 85.75] | 59.00 [44.50, 91.00] | 0.342 |
| Feature2 (median [IQR]) | 7.98 [5.30, 15.09] | 5.75 [4.22, 7.68] | 17.11 [14.60, 20.84] | <0.001 | 7.26 [5.17, 13.18] | 5.86 [4.71, 7.24] | 18.00 [12.96, 20.04] | <0.001 |
| Feature3 (median [IQR]) | 1.77 [1.29, 2.30] | 1.77 [1.25, 2.29] | 1.77 [1.35, 2.32] | 0.383 | 1.81 [1.38, 2.25] | 1.88 [1.38, 2.23] | 1.74 [1.39, 2.33] | 0.798 |
| Feature4 (median [IQR]) | 120.00 [68.50, 176.00] | 114.00 [72.50, 174.00] | 128.00 [65.50, 176.00] | 0.818 | 129.00 [64.00, 177.00] | 118.50 [62.25, 186.00] | 132.00 [91.50, 173.50] | 0.411 |
| Feature5 (median [IQR]) | 14.71 [6.85, 21.18] | 18.82 [15.62, 23.92] | 5.57 [4.18, 7.32] | <0.001 | 14.54 [7.30, 21.70] | 18.98 [14.65, 23.22] | 5.63 [4.44, 7.38] | <0.001 |
| Feature6 (median [IQR]) | 3.52 [2.24, 4.60] | 3.56 [2.30, 4.62] | 3.46 [2.08, 4.56] | 0.406 | 3.67 [2.48, 4.63] | 3.88 [2.67, 4.88] | 3.49 [2.02, 4.24] | 0.034 |
| Feature7 (median [IQR]) | 57.00 [41.00, 74.00] | 58.00 [37.50, 76.00] | 57.00 [43.75, 71.25] | 0.728 | 57.00 [38.00, 73.00] | 56.50 [39.25, 71.75] | 58.00 [34.50, 75.50] | 0.574 |
| Feature8 (median [IQR]) | 1.51 [0.85, 2.62] | 0.99 [0.65, 1.44] | 3.00 [2.48, 3.42] | <0.001 | 1.56 [1.07, 2.45] | 1.23 [0.79, 1.55] | 2.99 [2.42, 3.31] | <0.001 |
| Feature9 (median [IQR]) | 6.76 [4.50, 9.22] | 5.23 [3.51, 6.60] | 10.23 [8.96, 11.15] | <0.001 | 6.10 [4.11, 9.36] | 4.76 [3.34, 6.01] | 10.63 [9.31, 11.34] | <0.001 |
| Feature10 (median [IQR]) | 66.00 [44.00, 101.00] | 49.00 [38.00, 64.00] | 108.00 [99.75, 113.00] | <0.001 | 66.00 [42.00, 98.00] | 48.00 [36.00, 65.75] | 104.00 [98.00, 109.00] | <0.001 |
| HE4 (median [IQR]), pg/μg | 5.80 [2.40, 9.25] | 8.40 [6.10, 10.75] | 2.00 [1.40, 2.50] | <0.001 | 6.20 [2.30, 9.30] | 8.45 [6.35, 10.57] | 1.90 [1.50, 2.35] | <0.001 |
| ARF3 (median [IQR]), pg/μg | 20.70 [16.45, 67.20] | 17.80 [14.45, 20.30] | 74.15 [66.15, 86.93] | <0.001 | 20.20 [16.60, 71.90] | 18.00 [15.20, 20.20] | 76.50 [70.90, 88.90] | <0.001 |
| MYH10 (median [IQR]), pg/μg | 5.11 [3.70, 9.19] | 3.95 [3.11, 5.00] | 9.89 [8.90, 10.86] | <0.001 | 5.10 [3.70, 9.34] | 3.96 [3.36, 5.01] | 10.07 [9.32, 11.10] | <0.001 |

**Abbreviations**: IQR, Interquartile range; BMI, body mass index; COD, course of disease; LOL, location of lesion; GI, gynecological inflammation; CS, cervical stenosis; EFI, Endometriosis Fertility Index; AMH, anti-Müllerian hormone; CA125, carbohydrate antigen 125; Feature1, Wavelet.HLH_lbp.3D.m1_firstorder_kurtosis; Feature2, Wavelet.HLH_lbp.3D.m2_firstorder_kurtosis; Feature3, Roughness.index.of.boundary; Feature4, Original_shape_Elongation; Feature5, Original_firstorder_Skewness; Feature6, Original_glszm_SizeZoneNonUniformity; Feature7, Ipris_shell2_id_mean; Feature8, Original_firstorder_Kurtosis; Feature9, Normalized_radial_lengths_entropy; Feature10, Normalized_radial_lengths_mean.

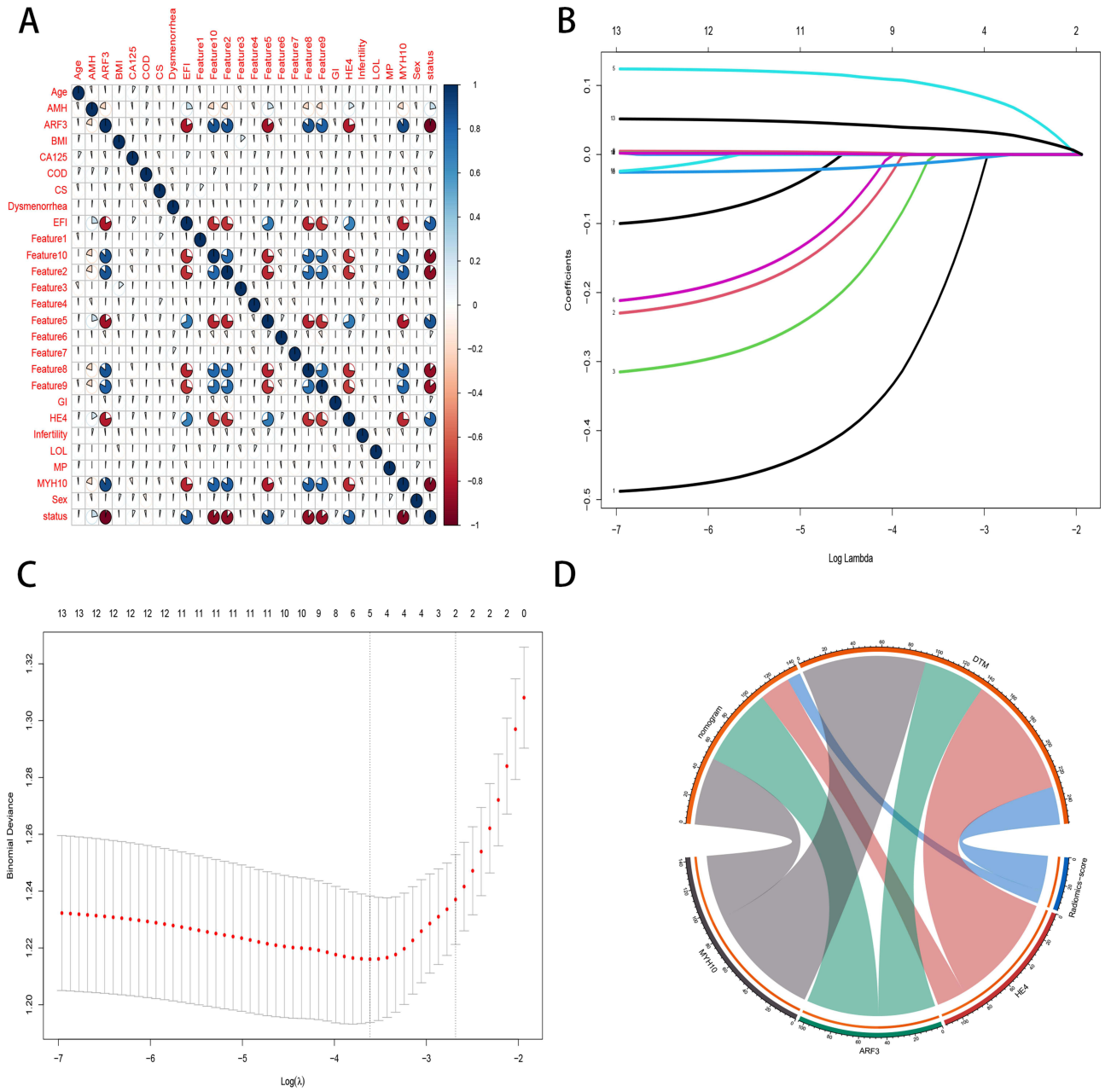


**Figure 2** Selection of candidate variables for predictive models (**A**) Pearson correlation coefficient analysis examines the correlation between candidate variables and outcome variables. (**B**) Recursive selection of optimal combination candidate predictor variables based on penalty coefficient. (**C**) Obtain candidate variable values for inclusion in the final prediction model based on the Lambda value. (**D**) Weight distribution of contribution values of candidate variables in two types of prediction models.

analyses, as shown in Figure 3B. The results indicate that the C-index can reach 0.816, indicating that the nomogram prediction model has extremely robust predictive performance.

## Construction of an Improved EFI Prediction Model Based on Decision Tree

As shown in Figure 4A, a decision tree prediction model based on candidate parameters was constructed. We used three candidate parameters for pruning to ultimately predict the likelihood of natural pregnancy outcomes. The decision tree was divided into four gradients, each with corresponding candidate parameters set for free random partitioning probabilities, and the final layer was considered as the natural pregnancy outcome. Meanwhile, as shown in Figure 4B, the decision tree model has a C-index of 0.776 in resampling, which was slightly less robust compared to nomogram.


https://doi.org/10.2147/IJGM.S512359

**Table 2** Univariate and Multivariate Logistic Regression Analysis of Risk Factors for EFI Natural Pregnancy Outcomes

| Variables | Univariate Analysis | | P-value | Multivariate Analysis | | P-value |
|---|---|---|---|---|---|---|
| | OR | 95% CI | | OR | 95% CI | |
| Radiomics score | 3.23 | 1.03–5.19 | <0.05 | 3.29 | 1.01–5.26 | <0.05 |
| HE4 | 2.88 | 0.76–3.55 | <0.05 | 2.87 | 0.79–3.78 | <0.01 |
| MYH10 | 1.54 | 0.21–3.08 | <0.05 | 1.29 | 0.33–3.47 | <0.01 |
| ARF3 | 2.14 | 0.99–3.78 | <0.05 | 2.17 | 1.01v4.51 | <0.05 |

**Abbreviations**: OR, odds ratio; 95% CI, 95% confidence interval.

## Evaluation of the Predictive Performance of Predictive Models

As shown in Table 3, the AUC values of nomogram in the training set and validation set were 0.921 (95% CI: 0.864–0.978) and 0.909 (95% CI: 0.852–0.966), respectively. However, the AUC values of the decision tree in the training and validation sets were 0.833 (95% CI: 0.776–0.890) and 0.817 (95% CI: 0.760–0.874), respectively. Additionally, the traditional EFI prediction model had AUC values of 0.889 (95% CI: 0.832–0.946) and 0.873 (95% CI: 0.816–0.930) in the training and validation sets, respectively. In addition, we evaluated the calibration of the model using Hosmer Lemeshow goodness-of-fit test, and the results showed that the internal validation set had a P-value of 0.881 and the external validation set had a P-value of 0.478 (both P>0.05), indicating good consistency of the model. Next, we evaluated the clinical utility of the DCA model and found that within the threshold probability range of 0.05–0.95, using the nomogram for predictive intervention in patients with EM had a higher net benefit compared to taking intervention measures for all patients (Figure 5A-B).

## Developing an Online Improved EFI Prediction Model for Clinical Application

Considering the superior predictive performance of the nomogram prediction model, we constructed an online visualization prediction model based on the *DynNom* software package, as shown in Figure 6A. All predicted variables were assigned online values, which means that patients with EM can evaluate the natural pregnancy probability after laparoscopic surgery by inputting the detected parameter values into the prediction model upon admission. At the same time, in order to evaluate the discriminative power of online prediction models, we evaluated the discriminative ability of online nomograms based on clinical impact curves (Figure 6B). The results showed that online nomograms (ie, improved EFI) have extremely accurate discriminative ability for EM patients with successful and failed natural pregnancies after surgery.

# Discussion

In recent years, the relationship between endometriosis and infertility has received widespread attention. According to statistics, 30% to 50% of endometriosis patients also suffer from infertility, and the probability of infertile women developing endometriosis is 6 to 8 times higher than that of normal women.[4,19] In fact, from ovulation and fertilization to implantation and development of the oosperm, endometriosis can cause certain effects, leading to infertility.[20,21]

EFI, proposed by Adamson et al in 2010, has become a widely recognized and widely used evaluation index for predicting the natural conception rate of EM patients after surgery.[10] A meta-analysis involving 4598 cases showed that patients with EFI scores of 0–2 had a cumulative natural pregnancy rate of 10% at 36 months after surgery, while women with EFI scores of 9–10 had a rate of 69%, and had the advantage of good prediction of natural pregnancy rates.[22] Retrospective studies in China also showed that patients with EFI scores of 8, 9, and 10 had cumulative pregnancy rates of 62.7%, 69.8%, and 81.1% at 36 months after surgery, respectively.[23] Patients with scores of 5–7 had a cumulative pregnancy rate of 44.4%, confirming that EFI has a good performance in predicting postoperative natural pregnancy rates.[24] However, EFI is a scoring system based on laparoscopic surgery, which carries risks such as anesthesia, bleeding, infection, adhesions, and postoperative ovarian dysfunction. It is also difficult to treat deep infiltrating endometriosis (DIE) during surgery, as the risk of damage to surrounding organs such as the intestine and bladder increases. There is also controversy over whether surgery can improve the success rate of IVF-ET in EM patients. Therefore, if accurate

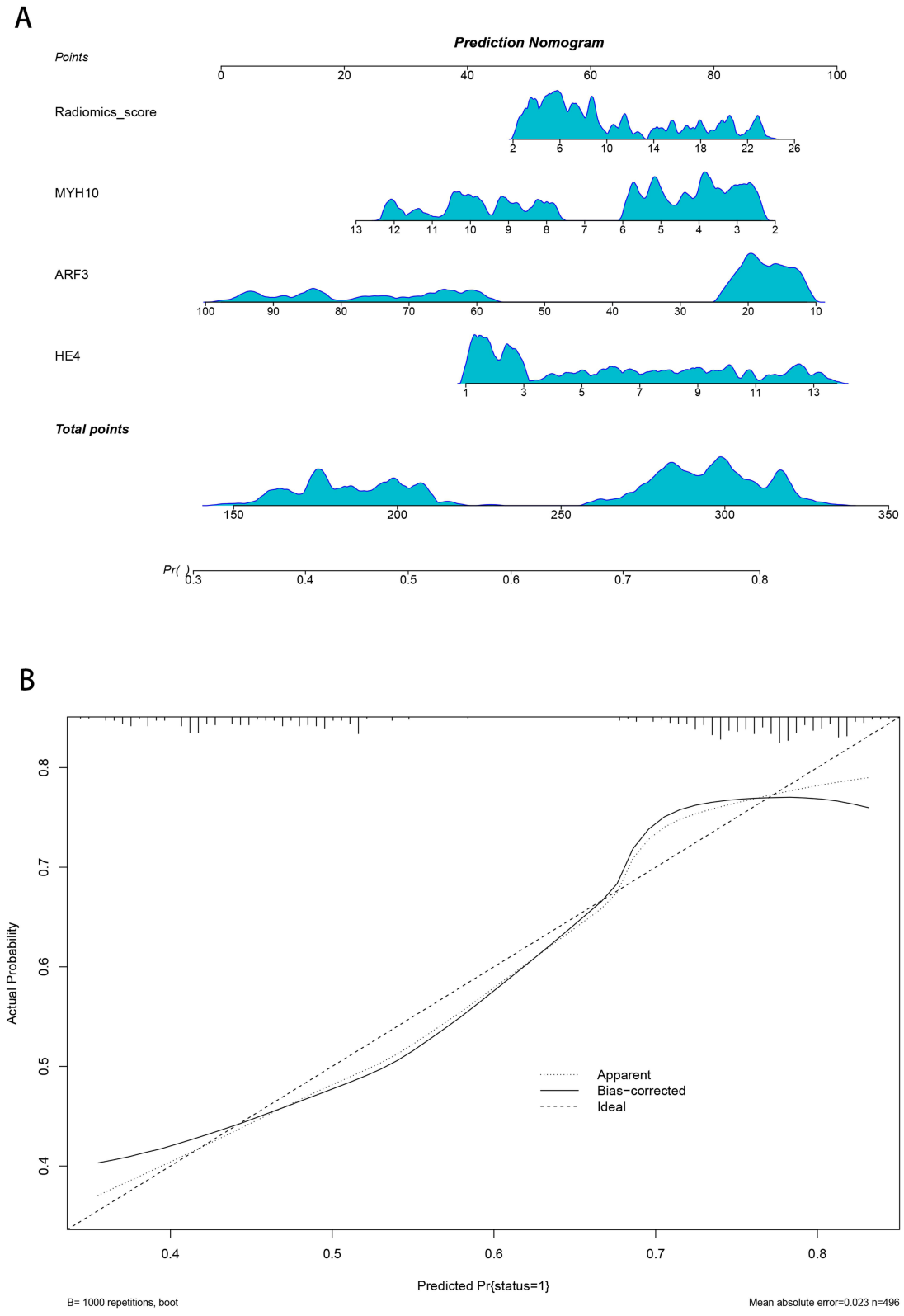


**Figure 3** Constructing an improved EFI prediction model based on nomogram visualization. (**A**) Nomogram; (**B**) Calibration curve.


https://doi.org/10.2147/IJGM.S512359

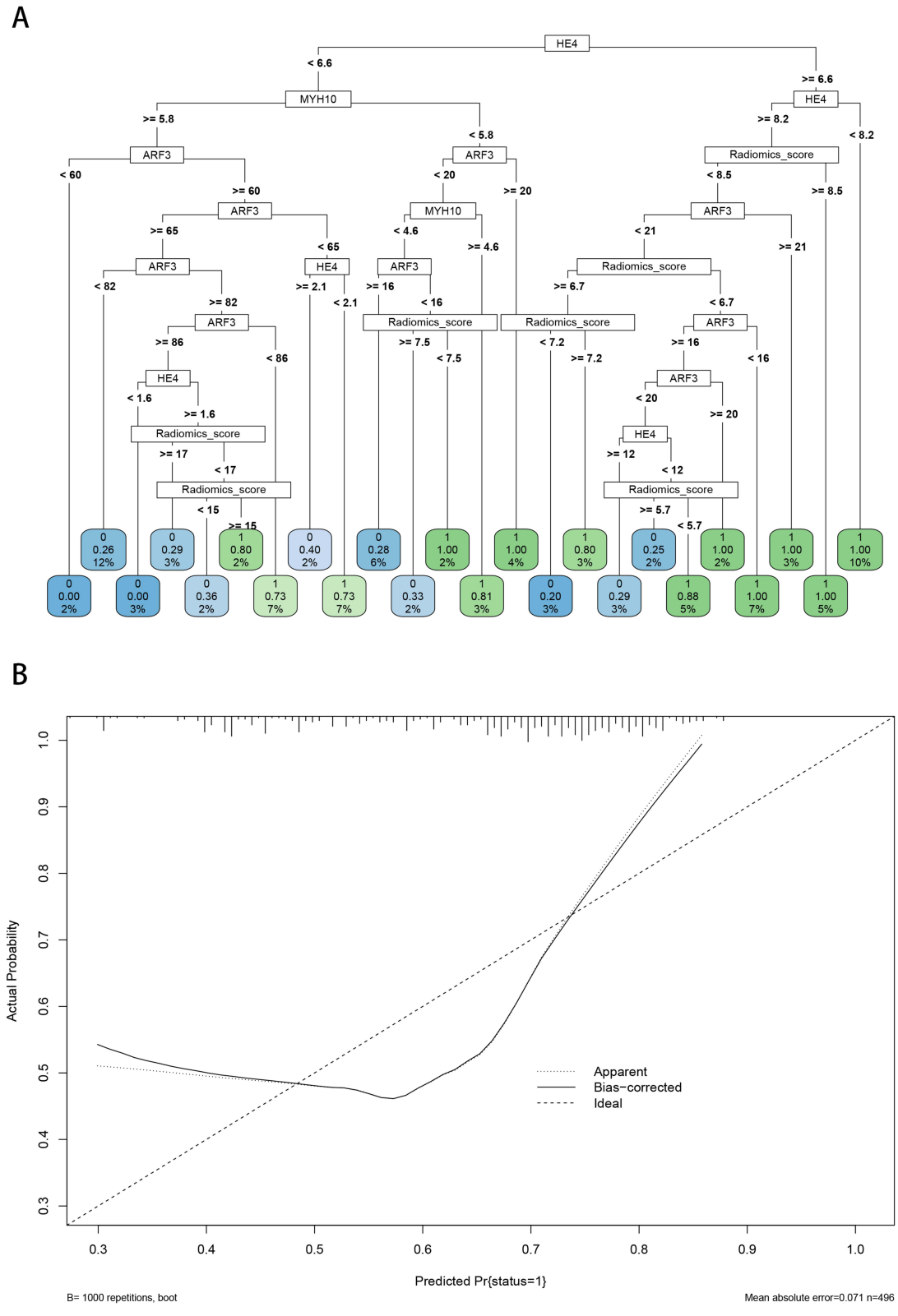


**Figure 4** Constructing an improved EFI prediction model based on decision tree visualization. (**A**) Decision tree model; (**B**) Calibration curve.

**Table 3** Efficiency Evaluation Model Based on the Area Under the Receiver Operating Characteristic

| Prediction Model | | Training Set | | | | Testing Set | | | |
|---|---|---|---|---|---|---|---|---|---|
| | | AUC | 95% CI | PPV | NPV | AUC | 95% CI | PPV | NPV |
| Improved EFI | Nomogram | 0.921 | 0.864–0.978 | 0.960 | 0.885 | 0.909 | 0.852–0.966 | 0.978 | 0.865 |
| | DTM | 0.833 | 0.776–0.890 | 0.887 | 0.812 | 0.817 | 0.760–0.874 | 0.854 | 0.901 |
| | EFI | 0.889 | 0.832–0.946 | 0.890 | 0.905 | 0.873 | 0.816–0.930 | 0.950 | 0.865 |

**Abbreviations**: AUC, area under the curve; 95% CI, 95% confidence interval; PPV, positive predictive value; NPV, negative predictive value; DTM, decision tree model.

predictions of EFI values are made based on clinical and imaging data, doctors can provide more personalized choices for patients and make decisions on their fertility management based on preoperative EFI scores.

There are two prerequisites for predicting EFI. Firstly, preoperative prediction of EM patients; Secondly, the surgical factors observed during laparoscopic surgery need to be transformed into a preoperative scoring system. Agarwal et al summarized a set of clinical diagnostic algorithms for EM based on symptoms, medical history, gynecological examinations, and auxiliary examinations.[25] We previously developed a nomogram for predicting EM in infertile patients, which showed the area under the curve of the model's EM prediction ability. The training sample was 0.780 and the validation sample was 0.750, emphasizing the importance of imaging in EM prediction. Therefore, with the development of imaging technology, the presence of EM can be better predicted preoperatively. In view of this, we hope to capture key information through texture feature analysis of ultrasound radiomics, in order to enhance the predictive ability of EFI.

In the past few decades, ultrasound technology has been widely used in the diagnosis of deep pelvic endometriosis, but there are few research reports on its use for pre - and post-operative fertility assessment of endometriosis.[26] In this study, we summarized and analyzed preoperative clinical and ultrasound data of EM patients, converted them into computable data, and formed a preoperative EFI scoring system. We used dimensionality reduction to extract eight omics features and constructed an improved EFI score to predict the probability of natural conception after surgery, with AUC values of 0.921 and 0.909 in the training and validation sets, respectively. Compared to the ultrasound parameters included in the EFI scoring system (including the maximum diameter of ovarian chocolate cysts indicated by ultrasound, whether there is hydrosalpinx, and whether there is deep infiltration), ultrasound imaging omics methods can automatically extract a large number of features, which help doctors gain deeper insights from medical images. In addition, this method reduces the subjective judgment bias of doctors, making the diagnosis more objective and consistent.

The application of urinary proteomics in endometriosis has shown certain potential and achievements. For example, the latest research indicates that the use of tandem mass labeling parallel reaction monitoring (TMT-PRM) proteomics technology has revealed elevated levels of histone 4 in the urine of patients with ovarian endometriosis, the results demonstrate that histone 4 has the highest diagnostic efficiency among endometriosis-specific peptides, with a sensitivity of 70% and specificity of 80%.[18] In the preliminary sequencing of urine proteomics results, we found significant statistical differences in natural pregnancy outcomes between EM patients and infertile patients in terms of histone 4, ARF3, and MYH10. Previous studies have shown that ARF3, as one of the subtypes of ADP ribosylation factor family, belongs to the same family as ARF1 and can participate in many important cellular functions, such as cell adhesion and migration.[27,28] In addition, ARF3 can also participate in NF-kB activation and cytokine production by regulating TLR9, while playing a key regulatory role in cytoplasmic motility.[29] MYH10, also known as non-muscle myosin II, is an excitatory protein binding protein that primarily constructs the cytoskeleton and participates in various activities including cytoplasmic motility, cell morphology regulation, cell adhesion, and cell migration.[30] It also maintains cell contractility, allowing cells to squeeze through the gaps in the basal layer and participate in cellular biological behavior. Encouraged by this, in this study, we constructed a panel using an ELISA kit and combined it with ultrasound radiomics to predict pregnancy outcomes with extremely high predictive power and robustness, which also opened up a new perspective for improving non-invasive prediction of EFI.

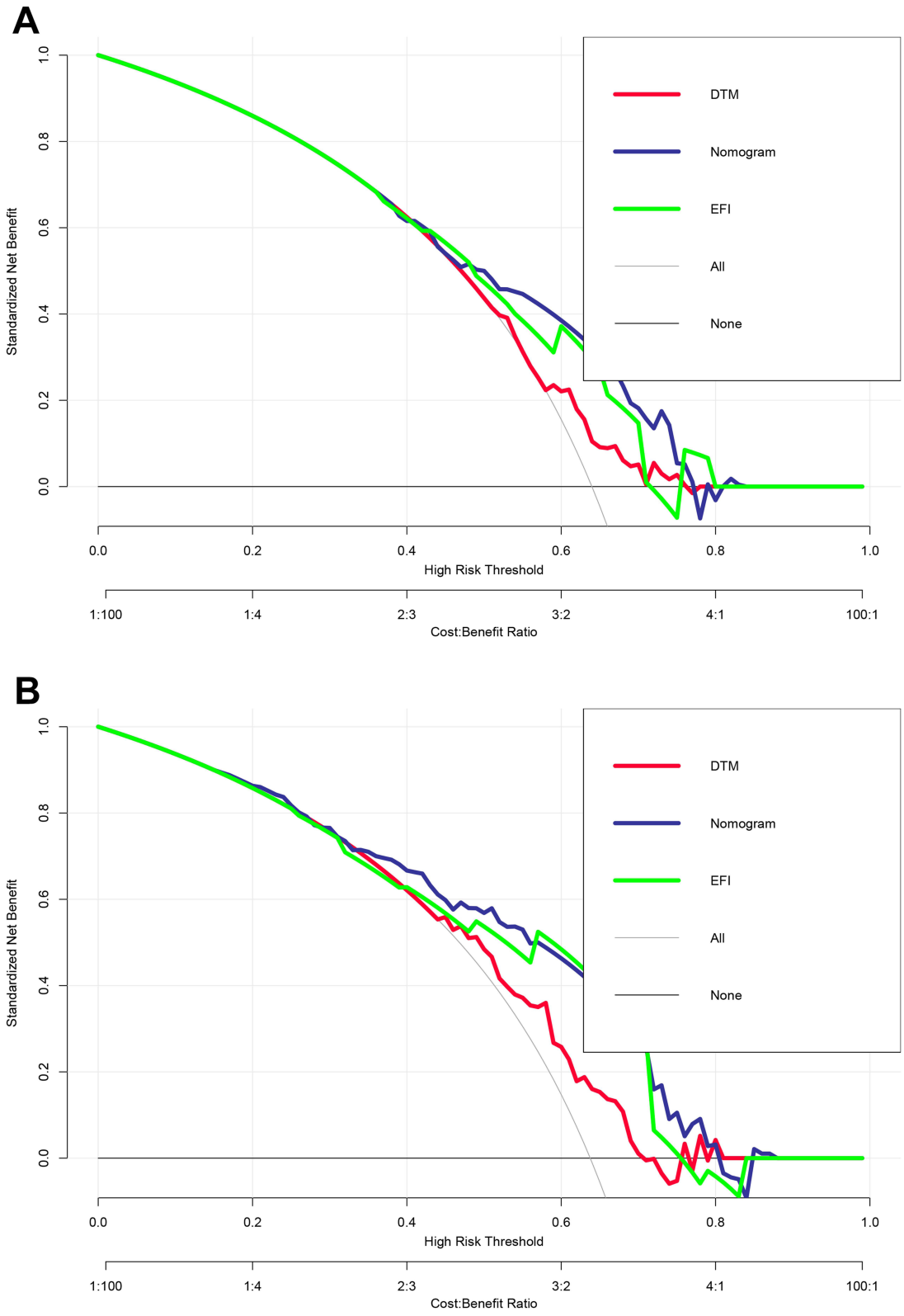


**Figure 5** Net benefit capability of improved EFI prediction model based on decision curve analysis. (**A**) Training cohort; (**B**) Testing cohort.


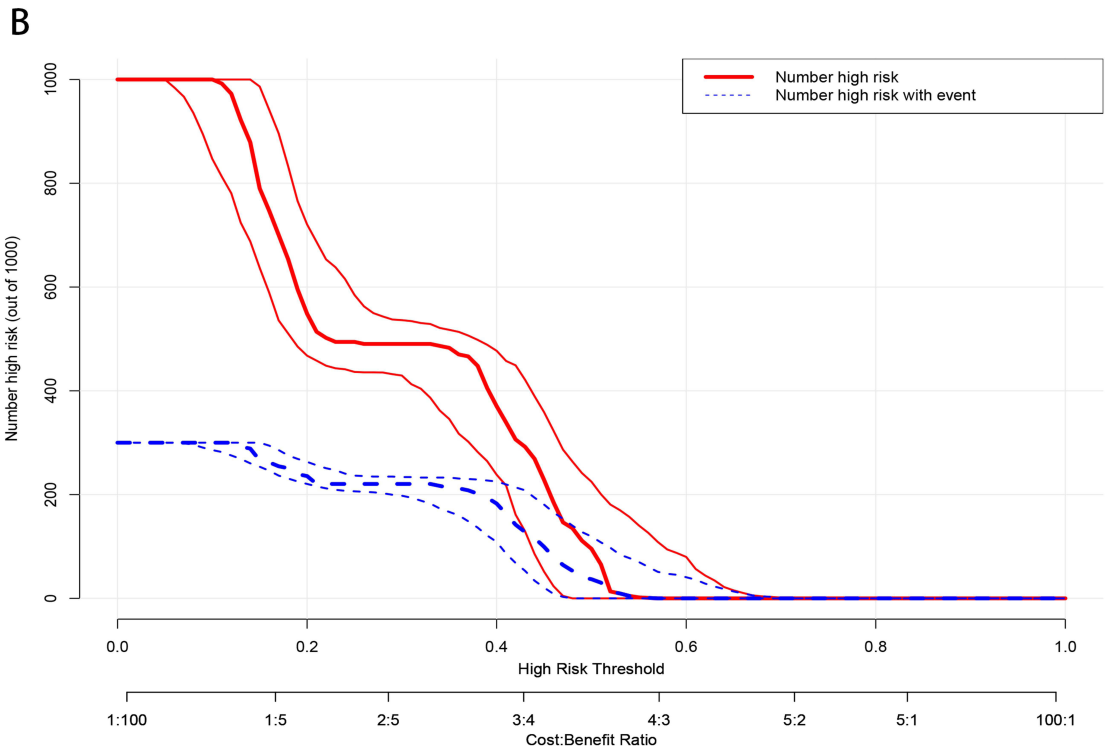


**Figure 6** Application of optimal improved EFI prediction model in clinical practice (**A**) Visualization of calculator prediction model. (**B**) Clinical impact curve. The impact curve of the predictive model's ability to distinguish between natural pregnancy and pregnancy failure. Among them, the red and blue lines represent two diseases respectively, and the farther apart they are, the better their ability to distinguish.


https://doi.org/10.2147/IJGM.S512359

Although we have successfully constructed an improved EFI scoring system, this study still inevitably has the following limitations. Firstly, as a predictive model for predicting the natural pregnancy outcomes of EM patients, this predictive model relies on high-level gynecological ultrasound and has strict requirements for the quality of ultrasound images. Therefore, training for ultrasound professionals is necessary before implementing EFI prediction. Secondly, this prediction model cannot replace laparoscopic surgery in guiding EM patients in reducing pelvic pain, improving pelvic environment, and enhancing quality of life. Therefore, further optimization is needed to increase the universality of the improved EFI prediction model. Thirdly, as a retrospective study, there is currently a lack of large-scale prospective multicenter validation, and further evaluation and revision are needed for its clinical application; Fourthly, although radiomics and uroproteomics have been successfully incorporated this time, it is still necessary to integrate multiple omics (such as transcriptomics) in the future to optimize the predictive ability of the prediction model.

## Conclusion

In summary, by incorporating ultrasound radiomics and urine proteomics, and utilizing machine learning algorithms, we have successfully constructed an improved EFI prediction scoring system. For infertile patients caused by EM, preoperative EFI score risk stratification and timely development of postoperative diagnosis and treatment strategies have important reference value for improving individualized pregnancy rates. In addition, the improved EFI parameter acquisition is easy to obtain and non-invasive, making it more suitable for promotion and practice on the clinical front line.

## Disclosure

The authors report no conflicts of interest in this work.

## References


1. Taylor HS, Kotlyar AM, Flores VA. Endometriosis is a chronic systemic disease: clinical challenges and novel innovations. *Lancet (London, England)*. 2021;397(10276):839–852. doi:10.1016/S0140-6736(21)00389-5
2. Allaire C, Bedaiwy MA, Yong PJ. Diagnosis and management of endometriosis. *CMAJ: Canadian Med Assoc J*. 2023;195(10):E363–e71. doi:10.1503/cmaj.220637
3. Crump J, Suker A, White L. Endometriosis: a review of recent evidence and guidelines. *Australian J General Pract*. 2024;53(1–2):11–18. doi:10.31128/AJGP/04-23-6805
4. Bonavina G, Taylor HS. Endometriosis-associated infertility: from pathophysiology to tailored treatment. *Front Endocrinol*. 2022;13:1020827. doi:10.3389/fendo.2022.1020827
5. Ferrero S. Endometriosis related infertility. *Best Pract Res Clin Obstet Gynaecol*. 2024;95:102504. doi:10.1016/j.bpobgyn.2024.102504
6. Penzias A, Azziz R, Bendikson K. Fertility evaluation of infertile women: a committee opinion. *Fertil Sterility*. 2021;116(5):1255–1265. doi:10.1016/j.fertnstert.2021.08.038
7. Chin AHB, Nguma JB, Ahmad MF. The American society for reproductive medicine's new and more inclusive definition of infertility may conflict with traditional and conservative religious-cultural values. *Fertil Sterility*. 2024;121(5):892. doi:10.1016/j.fertnstert.2023.12.019
8. Bortoletto P, Romanski PA, Lindheim SR, Pfeifer SM. The American society for reproductive medicine müllerian anomalies classification system: an updated framework with interactive tools. *J Minimally Invasive Gynecol*. 2022;29(7):820–822. doi:10.1016/j.jmig.2022.04.005
9. Tomassetti C, Bafort C, Meuleman C, Welkenhuysen M, Fieuws S, D'Hooghe T. Reproducibility of the Endometriosis Fertility Index: a prospective inter-/intra-rater agreement study. *BJOG: An Int J Obstet Gynaecol*. 2020;127(1):107–114. doi:10.1111/1471-0528.15880
10. Adamson GD, Pasta DJ. Endometriosis fertility index: the new, validated endometriosis staging system. *Fertil Sterility*. 2010;94(5):1609–1615. doi:10.1016/j.fertnstert.2009.09.035
11. Keckstein J, Hudelist G. Classification of deep endometriosis (DE) including bowel endometriosis: from r-ASRM to #Enzian-classification. *Best Pract Res Clin Obstet Gynaecol*. 2021;71:27–37. doi:10.1016/j.bpobgyn.2020.11.004
12. Tomassetti C, Bafort C, Vanhie A, et al. Estimation of the Endometriosis fertility index prior to operative laparoscopy. *Human Reprod*. 2021;36(3):636–646. doi:10.1093/humrep/deaa346
13. Jia Y, Yang J, Zhu Y, et al. Ultrasound-based radiomics: current status, challenges and future opportunities. *Med Ultrasonography*. 2022;24(4):451–460. doi:10.11152/mu-3248
14. Lambin P, Leijenaar RTH, Deist TM, et al. Radiomics: the bridge between medical imaging and personalized medicine. *Nat Rev Clin Oncol*. 2017;14(12):749–762. doi:10.1038/nrclinonc.2017.141
15. Rizzo S, Botta F, Raimondi S, et al. Radiomics: the facts and the challenges of image analysis. *Eur Radiol Exp*. 2018;2(1):36. doi:10.1186/s41747-018-0068-z
16. Bizzarri N, Russo L, Dolciami M, et al. Radiomics systematic review in cervical cancer: gynecological oncologists' perspective. *Int J Gynecol Cancer*. 2023;33(10):1522–1541. doi:10.1136/ijgc-2023-004589
17. Joshi N, Garapati K, Ghose V, Kandasamy RK, Pandey A. Recent progress in mass spectrometry-based urinary proteomics. *Clin. Proteomics*. 2024;21(1):14. doi:10.1186/s12014-024-09462-z
18. Chen X, Liu H, Sun W, Guo Z, Lang J. Elevated urine histone 4 levels in women with ovarian endometriosis revealed by discovery and parallel reaction monitoring proteomics. *J Proteomics*. 2019;204:103398. doi:10.1016/j.jprot.2019.103398

19. Coccia ME, Nardone L, Rizzello F. Endometriosis and Infertility: a Long-Life Approach to Preserve Reproductive Integrity. *Int J Environ Res Public Health*. 2022;19(10):6162. doi:10.3390/ijerph19106162
20. Tanbo T, Fedorcsak P. Endometriosis-associated infertility: aspects of pathophysiological mechanisms and treatment options. *Acta obstetricia et gynecologica Scandinavica*. 2017;96(6):659–667. doi:10.1111/aogs.13082
21. Filip L, Duică F, Prădatu A, et al. Endometriosis associated infertility: a critical review and analysis on etiopathogenesis and therapeutic approaches. *Medicina (Kaunas, Lithuania)*. 2020;56(9). doi:10.3390/medicina56090460.
22. Vesali S, Razavi M, Rezaeinejad M, Maleki-Hajiagha A, Maroufizadeh S, Sepidarkish M. Endometriosis fertility index for predicting non-assisted reproductive technology pregnancy after endometriosis surgery: a systematic review and meta-analysis. *BJOG: An Int J Obstet Gynaecol*. 2020;127(7):800–809. doi:10.1111/1471-0528.16107
23. Li X, Zeng C, Zhou YF, et al. Endometriosis Fertility Index for Predicting Pregnancy after Endometriosis Surgery. *Chinese Med J*. 2017;130(16):1932–1937. doi:10.4103/0366-6999.211892
24. Zhang X, Liu D, Huang W, Wang Q, Feng X, Tan J. Prediction of Endometriosis fertility index in patients with endometriosis-associated infertility after laparoscopic treatment. *Reprod Biomed Online*. 2018;37(1):53–59. doi:10.1016/j.rbmo.2018.03.012
25. Agarwal SK, Chapron C, Giudice LC, et al. Clinical diagnosis of endometriosis: a call to action. *Am J Clin Exp Obstet Gynecol*. 2019;220(4):354.e1–.e12. doi:10.1016/j.ajog.2018.12.039
26. Noventa M, Saccardi C, Litta P, et al. Ultrasound techniques in the diagnosis of deep pelvic endometriosis: algorithm based on a systematic review and meta-analysis. *Fertil Sterility*. 2015;104(2):366–83.e2. doi:10.1016/j.fertnstert.2015.05.002
27. Peterson AC, Russell JD, Bailey DJ, Westphall MS, Coon JJ. Parallel reaction monitoring for high resolution and high mass accuracy quantitative, targeted proteomics. *Molecular & Cellular Proteomics: MCP*. 2012;11(11):1475–1488. doi:10.1074/mcp.O112.020131
28. Casalou C, Faustino A, Barral DC. Arf proteins in cancer cell migration. *Small GTPases*. 2016;7(4):270–282. doi:10.1080/21541248.2016.1228792
29. Donaldson JG, Jackson CL. ARF family G proteins and their regulators: roles in membrane transport, development and disease. *Nat Rev mol Cell Biol*. 2011;12(6):362–375. doi:10.1038/nrm3117
30. Ma X, Adelstein RS. A point mutation in Myh10 causes major defects in heart development and body wall closure. *Circulation*. 2014;7(3):257–265. doi:10.1161/CIRCGENETICS.113.000455